Japanese Journal of Applied Physics

The Japan Society of Applied Physics

REGULAR PAPER

Optical detection of anisotropic *g*-factor and nuclear spin polarization in a single CdTe quantum well

To cite this article: Li-Ping Yan *et al* 2015 *Jpn. J. Appl. Phys.* **54** 033003

Japanese Journal of Applied Physics **54**, 033003 (2015) **REGULAR PAPER**
http://dx.doi.org/10.7567/JJAP.54.033003

Optical detection of anisotropic *g*-factor and nuclear spin polarization in a single CdTe quantum well

Li-Ping Yan[1], Masahiro Kurosawa[1], Wei-Ting Hsu[2], Wen-Hao Chang[2], and Satoru Adachi[1*]

[1]*Division of Applied Physics, Graduate School of Engineering, Hokkaido University, Sapporo 060-8628, Japan*
[2]*Department of Electrophysics, National Chiao Tung University, Hsinchu 300, Taiwan*
E-mail: adachi-s@eng.hokudai.ac.jp

Received December 11, 2014; accepted December 22, 2014; published online February 10, 2015

Longitudinal and in-plane electron *g*-factors, and a nuclear spin polarization (NSP) have been evaluated precisely in a CdTe/$Cd_{0.85}Mg_{0.15}Te$ single quantum well by using the time-resolved Kerr rotation and double lock-in detection techniques. Resident electron spin polarization (RESP) was formed via the negative trion formation and recombination, and RESP gave rise to NSP in an oblique magnetic field configuration. We observed the effective nuclear field of a few mT which was weak compared with that in III–V semiconductor nanostructures as expected, but the nuclear field can be converted to the maximal NSP of 12% in Faraday geometry.

1. Introduction

Resident electron spin polarization (RESP) in semiconductor nanostructures has gained considerable attention as one of key components in the potential applications of spin degree of freedom to electronic devices and quantum information processing because of the optical controllability and long spin coherence free from the recombination annihilation.[1–3] However, in practice, the large obstacle lies in creating RESP without any loss of polarization during the generation process. Therefore, a lot of research effort has been put forth to understand better the interaction of carrier spins with each other[4–6] and with their environments such as tunable lasers[7] or barrier layers.[8] Thanks to the previous studies, the generation dynamics of RESP in semiconductors has been clarified except for the initial temporal region.[1,9] One of the remained obstacles for a longer spin coherence is the hyperfine interaction (HFI) between the photo-created carriers and the lattice nuclei, which recently has attracted a great attention especially in quantum dots (QDs).[3] To suppress or avoid the influence of HFI for the utilization of a potential long carrier spin coherence, the use of hole spin instead of electron spin has been studied.[10,11] This is because the dipole–dipole type HFI that affects hole spins is believed to be considerably weaker than the contact-type HFI that affects electron spins. Alternative way is a choice of semiconductor materials consisting of isotopes with zero nuclear spin or low abundance isotopes with small quantum number of nuclear spins and small HF constants.

Here, we report on the precise measurements of longitudinal and in-plane electron *g*-factors and the detection of a nuclear spin polarization (NSP) in a naturally n-doped CdTe/$Cd_{0.85}Mg_{0.15}Te$ single quantum well (SQW). CdTe consists of the isotopes with $I_{Cd} = 1/2$, $p_{Cd} = 25\%$, $I_{Te} = 1/2$, $p_{Te} = 8\%$ and the other isotopes with $I_{Cd,Te} = 0$, where I_i, p_i are nuclear spin and natural abundance of the isotope *i*, respectively. Since II–VI semiconductors such as CdTe have generally small abundances of the isotopes with $I \neq 0$, the effect of HFI acting back on electron is expected to be 1 to 2 orders magnitude smaller than that in III–V counterparts such as InAs ($I_{In} = 9/2$, $p_{In} = 100\%$, $I_{As} = 3/2$, $p_{As} = 100\%$). Although II–VI nanostructures have such advantages, there are only a few reports to study the NSP in CdSe QDs[12–14] and CdTe QW.[15] To precisely evaluate the NSP in II–VI nanostructures, the accurate measurement of *g*-factors is required, which is one of key components for the above-mentioned applications. The time-resolved Kerr rotation (TRKR) and double lock-in detection techniques are employed in order to measure the *g*-factors precisely and to detect rather small NSP. Non-precessing stationary component of RESP along Larmor frequency vector was confirmed to be able to transfer the electron spin momenta to nonzero nuclear spins via HFI through a tilting angle dependence of external magnetic field. Consequently, we detected the effective nuclear field of a few mT and the NSP of 12% for a picosecond circularly polarized excitation with 10 mW in the oblique magnetic field of 170 mT at 9 K.

2. Experimental procedure

The sample used in this study is a naturally n-doped CdTe/$Cd_{0.85}Mg_{0.15}Te$ SQW with the well width of 30 monolayers (~100 Å) grown by molecular-beam epitaxy on a (001)-GaAs substrate. The sample was mounted in a cold-finger optical cryostat set at the center of a magnet, and was kept at ~9 K. The external magnetic field *B* up to ~450 mT could be applied at a variable tilting angle (+20 to −15°) to the sample surface. The sample was excited spin-selectively always by a normally incident σ^- (or σ^+)-polarized pump pulse via the optical transition selection rule. Similar to the standard TRKR setup, the linearly-polarized probe pulse with a controlled pump–probe delay time monitored the spin precession. Both the pump and probe were produced by a mode-locked Ti-doped sapphire laser (2 ps pulse width and 76 MHz pulse repetition rate). Typical averaged excitation powers were adjusted at ~10 mW for pump pulses and 0.5 mW for probe pulses. In order to evaluate precisely the longitudinal and transverse *g*-factors and the nuclear field B_N from the electron spin Larmor precession, the double lock-in detection[16] was combined with TRKR.

In the experiments, two kinds of modulation configurations were used. Setup I: only the pump beam was modulated by a photoelastic modulator (PEM) which was set at 50 kHz with a quarter wave retardation in phase. This modulation can change the pump polarization between σ^+ and σ^- eliminating the effect of B_N. Since the build-up time of B_N in a QW is much longer than the modulation period, the time-averaged zero electron spin population cannot create B_N. Setup II: the linearly polarized probe beam was modulated by a PEM set

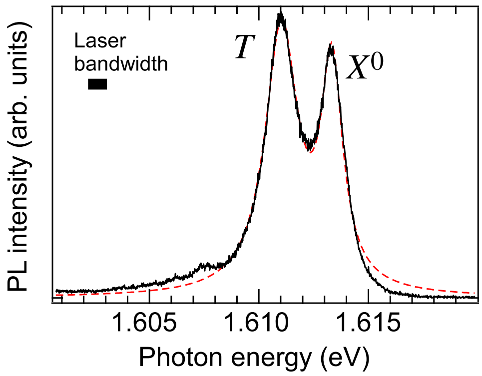

Fig. 1. (Color online) PL spectrum excited with 1.650 eV at 10 K and 0 mT in the studied CdTe/(CdMg)Te SQW. Negative trion (T) and neutral exciton (X^0) are clearly separated. Excitation laser bandwidth is also indicated by a bar.

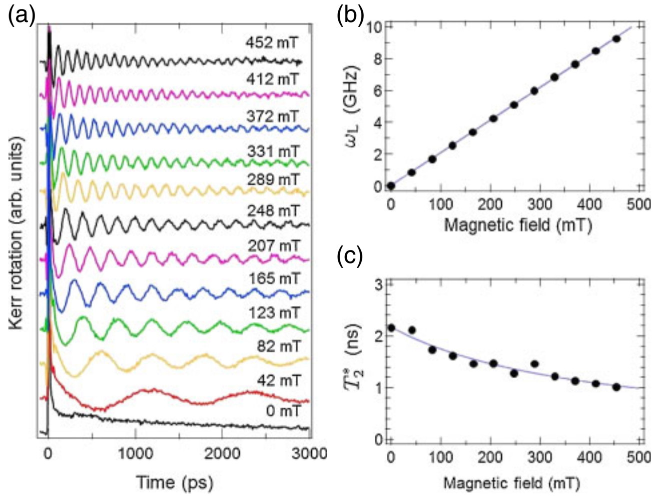

Fig. 2. (Color online) (a) Magnetic field strength dependence of TRKR signals $S_K(t)$ in Voigt geometry. (b) Observed Larmor frequencies in different field magnitude from 0 to 452 mT. (c) Dependence of T_2^* on the magnetic field. The solid curve indicates the expected values assuming the Gaussian distribution of g-factor with FWHM $\Delta g_\perp = 0.009$.

with a half-wave retardance at 50 kHz for lock-in detection. The circularly polarized pump beam generated by a quarter-wave plate was intensity-modulated by a mechanical chopper. In this case, the electron spin can create B_N depending on the B-direction.

Figure 1 shows the photoluminescence (PL) spectrum of this sample measured under cw-excitation at 1.650 eV and 10 K. From the excitation power and temperature dependences of PL spectra, the higher and lower energy peaks were found to be the neutral heavy-hole excitons (X^0, peak energy at 1.6133 eV) and the negative trions (T, peak energy at 1.6110 eV). Those peaks were clearly separated by the trion binding energy of 2.3 meV, which is comparable to the reported value of 2 meV for 200 Å CdTe QW.[1,2] Excitation wavelength in TRKR measurements was tuned to 769.6 nm in resonance with the trion transitions.

Optically excited electron–hole pairs capture additional electrons from the resident electron ensemble, and the negative trions T are formed in the ground state that consists of spin-singlet electron pair and a hole. This trion formation process polarizes the resident electron ensemble (i.e., RESP) since all the captured electron spins have to be opposite to the optically generated electron spins. After this process, the coherent RESP is modified by the hole spin relaxation in trion and trion recombination. The details of the trion dynamics are seen in Refs. 1, 2, and 9. For the purpose of this work, we focus on the signal behavior in the time region far after trion recombination time which was 85 ± 1 ps from the time-resolved PL measurement by a streak camera. In this time region, the observed long-lived precession is attributed unambiguously to the precession of RESP.

3. Results and discussion

3.1 g-factor measurements

Before discussing the nuclear field B_N, we firstly evaluate the electron g-factors in the growth direction ($g_\parallel$) and the in-plane direction ($g_\perp$) of the SQW under no effect of B_N. Therefore, the TRKR signals were measured in Setup I. Figure 2(a) indicates a set of TRKR signals generated by the σ^- pump pulse under $B = 0$–452 mT in Voigt geometry (i.e., at the zero tilting angle). Under the transverse magnetic field, RESP precesses with the Larmor frequency ω_L that is given by $\omega_L = g_\perp \mu_B B/\hbar$, where μ_B ($\sim$14 GHz/T) is a Bohr magneton and $\hbar$ is a reduced Planck's constant. The observed signal of RESP precession can be fitted well by an exponentially damped oscillation function containing the beating frequency ω_L and an initial phase ϕ;

$$S_K(t) = A^e \exp\left(-\frac{t}{T^*}\right)\cos(\omega_L t + \phi), \qquad (1)$$

where $S_K(t)$ corresponds to Kerr rotation angle of the probe pulse for recording the RESP precession, the coefficient A^e is the amplitude of RESP signal, t is the pump–probe delay, and T^* is the spin lifetime. The fitting was done for each TRKR signal in the time region of 500–3000 ps where only the resident electrons survive in the sample. T^* is given generally by $1/T^* = 1/T_1 + 1/T_2^*$ with the longitudinal relaxation time T_1 and the transverse spin relaxation time T_2^* for ensemble spins. In the case of the resident electrons, T_1 is infinity since they are free from the recombination annihilation, and therefore $T^* = T_2^*$. From the obtained signals, the ω_L increases linearly by $\omega_L(B)/(2\pi)$ (GHz) $= 0.02056B$ (mT) as shown in Fig. 2(b). Then, $|g_\perp| = 1.468 \pm 0.003$ is obtained, which is comparable to literature data measured by spin-flip Raman scattering method (1.49 ± 0.01 for non-doped 100 Å $CdTe/Cd_{0.75}Mg_{0.15}Te$ QW[17]) and TRKR method (1.64 for a modulation-doped 200 Å $CdTe/Cd_{0.78}Mg_{0.22}Te$ QW.[18]) The g-factor is determined basically by the material but varies by the wide variety of the band modulation: the well width, barrier height, doping, strain, etc.

Looking closer to the signal damping, the T_2^* of RESP is found to decrease from 2198 ps at 0 mT to 1016 ps at 452 mT as shown in Fig. 2(c). This reduction of T_2^* may originate from an effect of the macroscopic averaging of individual spin precessions with slightly different ω_L via the $g_\perp$ distribution, which is due to the fluctuations of well width and alloy composition of the barrier material. Assuming a Gaussian distribution of $g_\perp$ with the FWHM of $\Delta g_\perp$, the relation $1/T_2^*(B) = 1/T_2^*(0) + \Delta g_\perp \mu_B B/(\sqrt{2}\hbar)$ can be applied. From the experimental data, $\Delta g_\perp$ and $T_2^*(0)$ were estimated to be 0.009 and 2.2 ns.

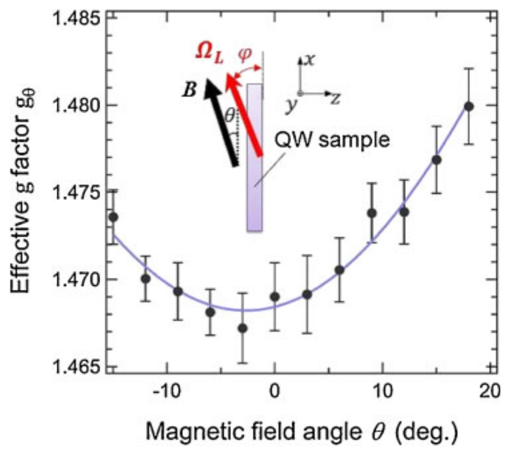

Fig. 3. (Color online) Effective g-factor g_θ of RESP measured by using a PEM with different tilted angle θ of the applied magnetic field. The solid line is a fitting curve by Eq. (2). Inset: schematic illustration of the oblique magnetic field geometry.

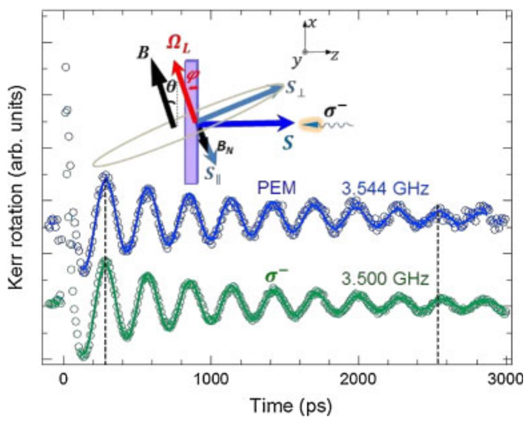

Fig. 4. (Color online) TRKR signals after PEM (upper) and σ^- (lower) pump excited at $\theta = 18°$, $B = 170\,\mathrm{mT}$, and 9 K. Inset: schematic illustration of tilted-field geometry under σ^- pump excitation with the tilted magnetic field by an angle of θ.

Even under the tilted magnetic field, there is no building-up of B_N via the σ^-/σ^+ alternating polarization excitation at 50 kHz provided by a PEM. Therefore, the Larmor frequency of RESP is decided by an effective g-factor g_θ and the external magnetic field without B_N. When the magnetic field B is applied in the x–z plane at an angle θ to the sample surface as shown in the inset of Fig. 3, $|g_\theta|$ is determined by the components of the g tensor along and normal to the plane as a following function:[19]

$$|g_\theta| = \sqrt{(g_\perp \cos\theta)^2 + (g_\parallel \sin\theta)^2}. \tag{2}$$

As shown in Fig. 3, the g_θ values obtained from the fitting of the TRKR curves under the constant field $B \sim 170\,\mathrm{mT}$ were varying between 1.468 and 1.480 with changing the tilted angle θ of the applied magnetic field. This means that g-factor has relatively large anisotropy $|g_\parallel| \neq |g_\perp|$. By using the relationship in Eq. (2) and the observed in-plane component ($|g_\perp| = 1.468 \pm 0.003$) as mentioned above, the g-factor perpendicular to the sample plane of $|g_\parallel| = 1.562 \pm 0.003$ can be evaluated. The value of $|g_\parallel|$ is comparable to the previous one (1.59 ± 0.01) in CdTe/(CdMg)Te QWs with the same well width and Mg-concentration.[17] Due to the anisotropic g-factors, an actual angle φ between the sample plane and the Larmor frequency vector $\Omega = \bar{g}_\theta \mu_B \boldsymbol{B}/\hbar$ is different from the magnetic field angle θ, which is slightly tilted away from the magnetic field direction, and the angle φ changes with the angle θ following the relation of $\tan\varphi = (g_\parallel/g_\perp)\tan\theta$. From the previous study,[17] both $g_\parallel$ and $g_\perp$ have the negative sign, and $g_\parallel/g_\perp > 0$.

3.2 Nuclear spin effect on the e-spin precession

In order to study the NSP produced by the contact-type HFI, TRKR measurements were performed through Setup II in the tilted field geometry which is shown in the inset of Fig. 4. In order to transfer the spin angular momenta from optically oriented electrons to the nuclear spins of lattice, it is necessary to make the parallel or anti-parallel component $S_\parallel$ of electron spin to Ω. After σ^- excitation, the component $S_\parallel$ of RESP gives rise to the dynamic nuclear polarization, i.e., the flip-flop term of HFI $(I^i_+ S_- + I^i_- S_+)/2$ between the i-th nuclear spin and electron spin. Subsequently, the resulting NSP produces a nuclear field (Overhauser field) B_N along a vector Ω and is observed via the energy shift by the static term $I^i_z S_z$.[3] However, since the created NSP precesses around the external magnetic field B, only the stationary component of B_N along B is effective to modify the RESP precession. As a result, the observed Larmor frequency $\bar{\omega}_L$ at which the transverse component $S_\perp$ of RESP rotates can be affected by both the applied field B and created nuclear field B_N, indicating the following function:

$$\bar{\omega}_L = g_\theta \mu_B (B \pm B_N)/\hbar. \tag{3}$$

The key feature is that the precession frequency is changed due to B_N, which can be indicated by the changing in the precession frequency of Kerr rotations for PEM and σ^- pumps in Fig. 4. The Larmor frequency for σ^- pump is reduced to 3.500 GHz from 3.544 GHz for σ^-/σ^+ (PEM) pump at $\theta = 18°$ and $B = 170\,\mathrm{mT}$. Note that, in the TRKR experiments using the σ^- pump pulses, the generated NSP reaches the saturated value within the time constant of the lock-in amplifier (typically 500 ms) and the saturated NSP has been already prepared in the negative time region since the σ^- pump pulses keep on exciting the electron spins.

Under the oblique magnetic field in the inset of Fig. 4, there are non-precessing spin component $S_\parallel$ and precessing component $S_\perp$ of the RESP in a TRKR signal. Therefore, the Kerr rotation angle $S_K(t)$ is expressed by the following function exhibiting two kinds of exponential decays:

$$S_K(t) = A^e_\parallel \exp\left(-\frac{t}{T^*_\parallel}\right) + A^e_\perp \exp\left(-\frac{t}{T^*_\perp}\right)\cos(\bar{\omega}_L t + \phi), \tag{4}$$

where the coefficients $A^e_\parallel$ and $A^e_\perp$ are the amplitudes corresponding to $S_\parallel$ and $S_\perp$, $T_\parallel$ and $T_\perp$ are the longitudinal and transverse spin relaxation times of RESP, respectively.

A set of TRKR curves like that in Fig. 4 have been measured via changing the direction of constant B of 170 mT. Then through Eq. (4), all the Larmor frequencies acquired from fitting of TRKR curves for σ^-/σ^+ (PEM) and σ^- excitations are shown in Fig. 5(a), which indicates that Larmor frequency could vary depending on the effective nuclear field and the changing g-factor induced by the tilted B direction. The Larmor frequency for σ^- pump decreases

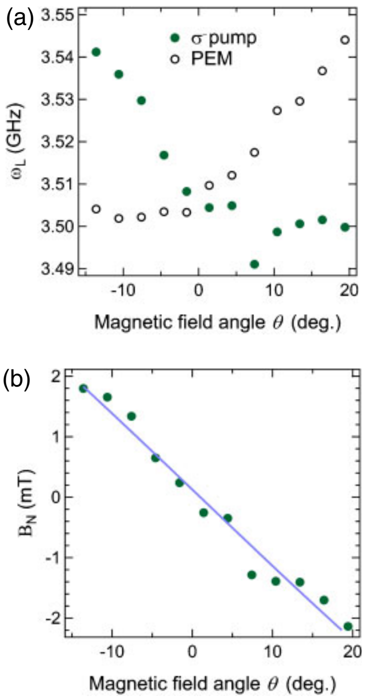

Fig. 5. (Color online) (a) Larmor frequencies of RESP measured for PEM-modulated and σ^- excitations at 9 K and $B = 170$ mT. (b) The nuclear field B_N and its trend-line as a function of the field angle θ.

with increasing the tilted angle from -15 to 18°. The difference between the frequencies by σ^-/σ^+ (PEM) and σ^- excitations corresponds to the frequency change due to the induced B_N, which is plotted as a function of the tilting angle in Fig. 5(b). Its absolute value tended to increase as the magnetic field angle increases. This is because the spin component $S_\parallel$, in proportion to $-\sin\theta$, increases with the increasing absolute inclination of applied magnetic field. Thus the maximum value of B_N for applying magnetic field perpendicular to the QW plane (i.e., Faraday configuration) would be B_N (90°) $= -7.3$ mT, which is similar to the reported values in CdTe QW[15] and bulk.[20] Nevertheless, this nuclear field is much weaker than the obtained value of 700 mT in GaAs/AlGaAs QWs.[21]

The maximum value of B_N along z-direction can be estimated by[3]

$$B_N^{\max} = \sum_i p_i A_i \langle I_i \rangle / (g_\parallel \mu_B), \tag{5}$$

where $\langle I_i \rangle$ is the mean spin of the nucleus i (= Cd, Te) and A_i is the contact-type HFI constant for each species ($A_{Cd} = -31\,\mu$eV and $A_{Te} = -45\,\mu$eV) weighted by the overlap between electronic and nuclear wavefunctions. Thus, the maximum value of $B_N^{\max}$ in Faraday geometry was expected to be ~63 mT with the obtained $|g_\parallel| = 1.562$. Therefore, the measured degree of NSP ($\langle I_i \rangle / I$) will be 12% under the longitudinal magnetic field. Although the generated B_N is very small compared to that in the III–V semiconductors such as GaAs and InAs, the converted degree of NSP is comparable to $\langle I_i \rangle / I \sim 30\%$ in III–V semiconductor QDs[22] and is far beyond the value in thermal equilibrium. Since the spin selective excitation induces the generation of B_N inherently, the use of the II–VI semiconductor materials has an advantage to the suppression of the effect of the nuclear field.

4. Summary

In summary, the NSP was created by the HFI between nuclei spins and RESP after optically polarized negative trion generation in a CdTe/$Cd_{0.85}Mg_{0.15}Te$ SQW and the resultant small nuclear field was detected by using TRKR technique. In addition, the longitudinal and transverse electron g-factors were deduced precisely. The created B_N was just around an order of a few mT, which was much weaker than the value obtained in III–V semiconductor nanostructures. The converted NSP was achieved up to 12%. The small effect of the nuclear field is preferred for spintronic devices which require the spin manipulation at rather low magnetic fields.

Acknowledgements

We gratefully thank G. Karczewski (Institute of Physics, Polish Academy of Sciences) for the sample growth. We also thank S. Takeyama (Institute for Solid State Physics, University of Tokyo) for fruitful discussions. Part of this work has been supported by JSPS KAKENHI Grant Number 22310063. Also, the China Scholarship Council is acknowledged for the studentship financial support at Hokkaido University.

1) E. A. Zhukov, D. R. Yakovlev, M. Bayer, M. M. Glazov, E. L. Ivchenko, G. Karczewski, T. Wojtowicz, and J. Kossut, Phys. Rev. B **76**, 205310 (2007).
2) G. V. Astakhov, M. M. Glazov, D. R. Yakovlev, E. A. Zhukov, W. Ossau, L. W. Molenkamp, and M. Bayer, Semicond. Sci. Technol. **23**, 114001 (2008).
3) *Spin Physics in Semiconductors*, ed. M. I. Dyakonov (Springer, Berlin, 2008) Chaps. 3, 4, and 6.
4) A. Tackeuchi, T. Kuroda, S. Muto, Y. Nishikawa, and O. Wada, Jpn. J. Appl. Phys. **38**, 4680 (1999).
5) S. L. Lu, H. Nosho, A. Tackeuchi, L. F. Bian, J. R. Dong, and Z. C. Niu, Jpn. J. Appl. Phys. **48**, 100206 (2009).
6) R. T. Harley, M. A. Brand, A. Malinowski, O. Z. Karimov, P. A. Marsden, A. J. Shields, D. Sanvitto, D. A. Ritchie, and M. Y. Simmons, Physica E **17**, 324 (2003).
7) P. Palinginis and H. Wang, J. Magn. Magn. Mater. **272–276**, 1919 (2004).
8) W. Shichi, T. Ito, M. Ichida, H. Gotoh, H. Kamada, and H. Ando, Jpn. J. Appl. Phys. **48**, 063002 (2009).
9) L.-P. Yan, M. Kurosawa, R. Kaji, G. Karczewski, S. Takeyama, and S. Adachi, Phys. Rev. B **90**, 205307 (2014).
10) B. Eble, C. Testelin, P. Desfonds, F. Bernardot, A. Balocchi, T. Amand, A. Miard, A. Lemaitre, X. Marie, and M. Chamarro, Phys. Rev. Lett. **102**, 146601 (2009).
11) R. Kaji, S. Ohno, T. Hozumi, and S. Adachi, J. Appl. Phys. **113**, 203511 (2013).
12) I. A. Akimov, D. H. Feng, and F. Henneberger, Phys. Rev. Lett. **97**, 056602 (2006).
13) J. Kim, J. Puls, Y. S. Chen, G. Bacher, and F. Henneberger, Appl. Phys. Lett. **96**, 151908 (2010).
14) C. Le Gall, A. Brunetti, H. Boukari, and L. Besombes, Phys. Rev. B **85**, 195312 (2012).
15) C. Testelin, B. Eble, F. Bernardot, G. Karczewski, and M. Chamarro, Phys. Rev. B **77**, 235306 (2008).
16) A. Kanno and Y. Masumoto, J. Lumin. **119–120**, 178 (2006).
17) A. A. Sirenko, T. Ruf, M. Cardona, D. R. Yakovlev, W. Ossau, A. Waag, and G. Landwehr, Phys. Rev. B **56**, 2114 (1997).
18) E. A. Zhukov, D. R. Yakovlev, M. Bayer, G. Karczewski, T. Wojtowicz, and J. Kossut, Phys. Status Solidi B **243**, 878 (2006).
19) G. Salis, D. Awschalom, Y. Ohno, and H. Ohno, Phys. Rev. B **64**, 195304 (2001).
20) A. Nakamura, D. Paget, C. Hermann, C. Weisbuch, G. Lampel, and B. C. Cavenett, Solid State Commun. **30**, 411 (1979).
21) A. Malinowski and R. T. Harley, Solid State Commun. **114**, 419 (2000).
22) For example, R. Kaji, S. Adachi, H. Sasakura, and S. Muto, Phys. Rev. B **85**, 155315 (2012).